5-2010

Observing and modeling the nocturnal park cool island of an arid city: Horizontal and vertical impacts

Winston T. L. CHOW
Singapore Management University, winstonchow@smu.edu.sg

Ronald L. POPE

Anthony J. BRAZEL

Citation

CHOW, Winston T. L., POPE, Ronald L., & BRAZEL, Anthony J..(2010). Observing and modeling the nocturnal park cool island of an arid city: Horizontal and vertical impacts. *Theoretical and Applied Climatology, 103(1)*, 197-211.

Available at: https://ink.library.smu.edu.sg/soss_research/3067

Theor Appl Climatol
DOI 10.1007/s00704-010-0293-8

ORIGINAL PAPER

Observing and modeling the nocturnal park cool island of an arid city: horizontal and vertical impacts

Winston T. L. Chow · Ronald L. Pope · Chris A. Martin · Anthony J. Brazel

Received: 27 July 2009 / Accepted: 4 May 2010

Abstract We examined the horizontal and vertical nocturnal cooling influence of a small park with irrigated lawn and xeric surfaces (~3 ha) within a university campus of a hot arid city. Temperature data from 0.01- to 3-m heights observed during a bicycle traverse of the campus were combined with modeled spatial temperature data simulated from a three-dimensional microclimate model (ENVI-met 3.1). A distinct park cool island, with mean observed magnitudes of 0.7–3.6°C, was documented for both traverse and model data with larger cooling intensities measured closer to surface level. Modeled results possessed varying but generally reasonable accuracy in simulating both spatial and temporal temperature data, although some systematic errors exist. A combination of several factors, such as variations in surface thermal properties, urban geometry, building orientation, and soil moisture, was likely responsible for influencing differential urban and non-urban near-surface temperatures. A strong inversion layer up to 1 m over non-urban surfaces was detected, contrasting with near-neutral lapse rates over urban surfaces. A key factor in the spatial expansion of the park cool island was the advection of cooler park air to adjacent urban surfaces, although this effect was mostly concentrated from 0- to 1-m heights over urban surfaces that were more exposed to the atmosphere.

W. T. L. Chow (✉) · A. J. Brazel
School of Geographical Sciences and Urban Planning,
Arizona State University,
P.O. Box 875302, Tempe, AZ 85287-5302, USA
e-mail: wtchow@asu.edu

R. L. Pope
School of Life Sciences, Arizona State University,
Tempe, AZ, USA

C. A. Martin
Department of Applied Sciences and Mathematics,
Arizona State University,
Mesa, AZ, USA

1 Introduction

Parks and other green spaces located within cities generally have lower surface and ambient air temperatures compared to typical urban surfaces such as concrete, tarmac, and asphalt (e.g., Jauregui 1990/1991; Saito et al. 1990/1991). This is primarily due to alterations to the surface energy balance, with relatively more radiant energy partitioned into the latent heat and/or heat storage terms as opposed to sensible heat (Oke 1987). Other reasons why parks/green spaces might be cooler than the surrounding structures include the greater direct shading from vegetation with large canopies that reduces surface temperatures, a higher sky view factor relative to urban surfaces allowing for unimpeded radiative cooling to the sky, and a lack of heat from combustion sources (Spronken-Smith and Oke 1999; Shashua-Bar et al. 2009).

This phenomenon of patchy, cooler areas within the urban mosaic is often termed the park cool island (PCI). Increasingly, urban planners are aware that managed PCIs through the use of urban green spaces could be a useful applied tool towards mitigating detrimental impacts stemming from the urban heat island (UHI), especially within tropical and sub-tropical cities of large spatial extent (e.g., Emmanuel 2005). Past research of PCI effects mostly relied on observational studies focusing on the spatial distribution of temperatures with respect to adjacent urban surroundings, with much fewer studies either examining the vertical form of PCI or modeling the impacts of green spaces on the urban environment.

Published online: 21 May 2010

In this study, we examined both horizontal and vertical nocturnal temperature differences at different heights between a non-urban, largely vegetated surface and its urban surroundings. We analyzed horizontal micro-scale temperature fields and vertical (i.e., lapse rate) profiles within a study area located in an arid desert climate. We obtained PCI intensities through two methods: (a) direct, relatively high frequency (1 s) temperature measurements obtained from a bicycle traverse over different land use types and (b) modeling study area temperatures through a three-dimensional numerical micro-meteorological model (ENVI-met 3.1) with inputs adapted to local soils and vegetation. A secondary objective was to evaluate the accuracy of modeled vs. observed temperatures from the traverse and a nearby meteorological station. This study aims to improve the understanding of PCI effects for a desert city, of which research is relatively deficient compared to other urban climates.

2 Literature review

PCI can be measured either through surface or air temperature differences between urban surroundings with the park or green space (ΔT_{u-p}). Distinct differences of surface temperatures between parks and adjacent urban areas often result in dynamic variations of $\Delta T_{u-p(surface)}$ (Roth et al. 1989). Variations of $\Delta T_{u-p(air)}$ are strongly coupled with underlying surface types at micro-scales, although greater turbulence and advection reduce magnitudes of surface air thermal coupling, especially at distinct borders between surface types at micro-scale levels (Jansson et al. 2007). Higher wind speeds and the resulting local-scale turbulent mixing also dilutes the maximum magnitude of $\Delta T_{u-p(air)}$ relative to $\Delta T_{u-p(surface)}$ and may also expand the influence of the PCI beyond the physical boundaries of the park (Oke 1989; Eliasson and Upmanis 2000). Magnitudes of mean $\Delta T_{u-p(air)}$ range from 1.5 to 4°C (Sham 1987; Upmanis et al. 1998; Jonsson 2004), but maximum intensities can be as large as ~7°C during summer nocturnal periods in Sacramento, CA, USA (Spronken-Smith and Oke 1998).

The size of the park or green space, topography, wind speeds, and vegetation types are factors influencing PCI magnitudes and development. Larger parks are generally associated with greater PCI intensities (Barradas 1991; Jauregui 1990/1991), and magnitudes of $\Delta T_{u-p(air)}$ inversely correlate to wind speeds (Spronken-Smith 1994). Topographic variations potentially affect regional airflow into parks at different spatial scales, such as by large-scale nocturnal katabatic drainage from mountains to a valley city that reduces urban air temperatures adjacent to parks (Kirby and Sellers 1987). Vegetation types in parks also affect the timing of maximum PCI (Spronken-Smith and Oke 1998), with (a) parks with substantial tree canopies having greatest cooling impacts during the afternoon, (b) mixed use, garden, or savannah parks having PCI maxima around sunset, and (c) open grass parks having observed PCI maximums around sunrise.

Of particular interest are geographical differences in ΔT_{u-p} within cities located in hot arid vs. other climates. The scarcity of surface and atmospheric moisture, combined with intense diurnal surface radiative exchanges, is a significant qualitative difference affecting PCI development in desert cities (Pearlmutter et al. 2007). Latent heat fluxes from surface evapotranspiration in desert cities are much lower relative to urban areas in other climates, but this strongly depends on irrigation availability for parks in these cities. For instance, daytime summer latent heat fluxes in Tucson, AZ, USA, where landscape irrigation of suburban residential green spaces is prevalent, accounted for 25–35% of the daytime surface energy balance (Grimmond and Oke 1995). In contrast, a similar contribution to the surface energy balance of Mexicali, Mexico, which lacked water availability for irrigation, was only ~10% (Garcia-Cueto et al. 2003). Irrigation of green spaces is therefore important for daytime cooling through evapotranspiration within desert cities (e.g., Pearlmutter et al. 2009), especially combined with windy conditions that expand the “oasis effect” of PCI (Spronken-Smith et al. 2000). Increases in surface and soil moisture from irrigation also alter the surface thermal admittance of parks (μ), an important property measuring the ability of a surface to accept or release heat (Oke 1987). Higher (lower) soil moisture content results in higher (lower) μ, resulting in reduced (increased) urban vs. green space near-surface temperature differences (Chow and Roth 2006). As nocturnal park cooling appears to be more dependent on surface conduction and radiation processes as opposed to evapotranspiration (Oke et al. 1991; Spronken-Smith and Oke 1999), the timing of irrigation of parks post-sunset potentially affects diurnal PCI development and nocturnal PCI intensities in arid cities.

The study of PCI impacts within arid urban areas is important, given the increasing population and urban development seen in several Middle-Eastern and North American desert cities in recent years, including Phoenix, AZ, USA (Gober 2006). It is also essential to examine the methods and techniques of cooling urban landscapes (e.g., Shashua-Bar et al., 2009), which include increasing and maintaining urban green spaces. It is thus unsurprising that urban parks have a great potential in mitigating detrimental nocturnal UHI impacts in desert cities, as well as reducing overall urban energy consumption (Kurn et al. 1994), especially if urban vegetation are well maintained (Muellar and Day 2004). In Phoenix, the placement, design and upkeep of urban green spaces are important in reducing UHI intensities and in potentially improving human health and quality of life without excessively consuming natural resources. Thus, they are a key component in developing sustainable urban landscapes for this large metropolitan area (Stabler et al. 2005; Martin 2008).

Previous study methodologies investigating on the thermal impacts of urban parks generally used data obtained from station temperatures and/or vehicular traverses (e.g., Sham 1987; Upmanis et al. 1998; Jonsson 2004) or through hardware scale modeling (Spronken-Smith and Oke 1999; Pearlmutter et al. 2009). These methods usually focus on examining both spatial form and intensities of ΔT_{u-p} across different urban land use types. Much fewer studies (e.g., Jansson et al. 2007), however, examine the vertical impacts of PCI, i.e., analyze temperature profiles or lapse rates over different surface types within the urban canopy layer (i.e., from surface to mean roof height). Compared to these research methods, there has also been hitherto less work into modeling ΔT_{u-p}, especially at micro-spatial scales (i.e., linear and areal extents ranging from approximately 1 to 10^2 m or m^2) (Oke, 2004). Some research of micro-scale numerical modeling of urban vegetation impacts exist, although these are limited to simulations adding individual street trees in Colombo, Sri Lanka, and in downtown Phoenix (Emmanuel and Fernando 2007) or via increasing rooftop or vertical vegetation density in Singapore (Wong and Jusof 2008).

3 Materials and methods

3.1 Study area

The study was conducted in the Tempe campus of Arizona State University, located within the Phoenix metropolitan area (33.416° N, 111.931° W, 355.4 m above sea level). A 23-ha section of the campus centered on the Student Recreation Complex (SRC) field was selected as our study area (Fig. 1). The ~3-ha-sized field is a level urban green space mostly covered by lawn grass (0.05–0.1-m heights) of either bermuda (summer) or rye (winter) species, which are similar to grasses used for residential landscaping throughout suburban Phoenix. Parts of the field were exposed bare sandy–loam soil, especially in the center and along three of its four corners. The field was bounded by a wide variety of medium height trees (5–10 m) (e.g., Seville sour orange, *Citrus aurantium*, and Chinese pistache, *Pistacia chinensis*) with a wide canopy and dense foliage along the north, south, and east field perimeters and by taller trees (20–25 m) (e.g., coolibah, *Eucalyptus microtheca*, and Mexican fan palm, *Washingtonia robusta*) along the west field perimeter. Other smaller lawn grass plots with medium-height trees of similar height, e.g., blue palo verde (*Parkinsonia florida*), southern live oak (*Quercus virginiana*), and desert fan palm (*Washingtonina filifera*), lined several roads and boulevards, especially on the northern and southern boundary areas. These vegetation species are also commonly found in residential areas for landscaping. Buildings in the study area varied between 5 and 30 m above surface level (a.s.l.), with a mean height of ~10 m. A section of several hardcourt tennis courts and an Olympic-sized swimming pool were located to the west and south of the field.

Using ArcView 9.3 GIS, we created a three-dimensional (3-d) model by digitizing an aerial photograph of the study area as well as from fieldwork reconnaissance (Fig. 1). This model was subsequently used in traverse route design (Fig. 2), with the objective of extensive temperature sampling coverage over different surface types, such as urban (e.g., asphalt, concrete, and tennis court) and non-urban (e.g., xeric and lawn grass) surfaces categorized within the study area. In addition, temperatures on surfaces confined within a street or pavement canyon between buildings (i.e., urban canyons) were classed in a separate category. To quantify the aspect ratio of building height vs. spacing in these urban canyons, sky view factors were estimated using 3DSkyView, an ArcView 3.2 GIS program extension written by Souza et al. (2003). This program has been shown to produce more accurate results than other geometric estimation techniques, with similar, if slightly elevated, results when compared with actual field data. Minimum (mean) sky view factors in these canyons were 0.5 (0.7), indicating low- to medium-density urban development in the study area.

3.2 Observed temperature data

An instrument setup similar to Sun et al. (2009) was utilized to obtain and geo-code spatial temperature data. We used the TR-72U temperature/relative humidity sensor–datalogger (T&D Corporation), which had a specified resolution (accuracy) of 0.1°C (± 0.3°C), and the BT-Q1000 GPS travel recorder (Qstarz) which noted geographical coordinates of latitude, longitude, and altitude with a reacquisition rate of ~1 s. Four TR-72U sensors were attached to a metal pole before being vertically mounted to a bicycle at 0.01-, 1-, 2-, and 3-m heights a.s.l. As these sensors were not aspirated, it was also important that measurements occurred when the air was not completely stagnant during the study to minimize lags in sensor response. The GPS system was also attached to the pole to record geographical coordinates of every temperature sampling point. Each TR-72U sensor and the Q1000 recorder were synchronized and programmed to sample temperatures and geographical coordinates at 1-s intervals.

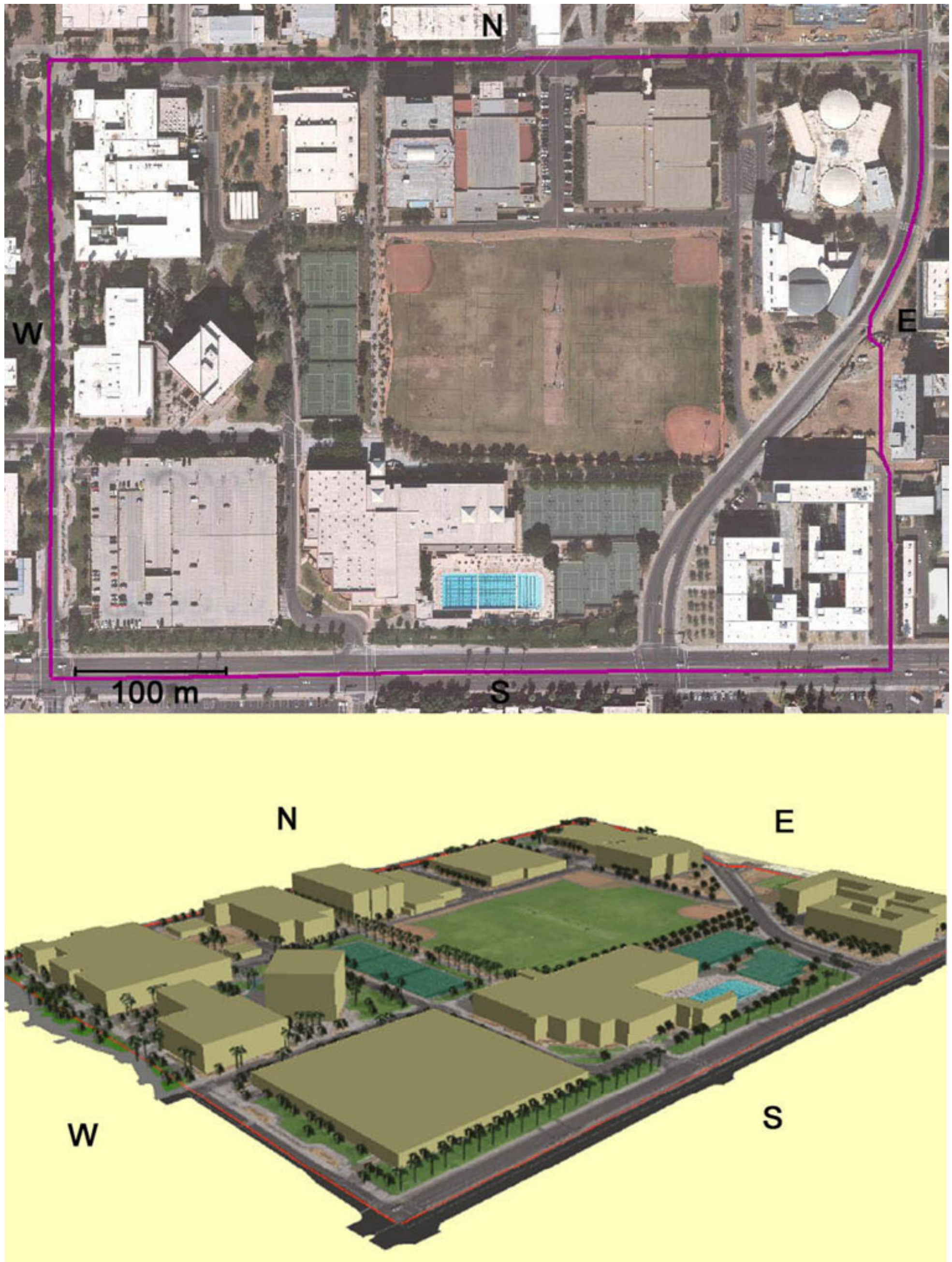

Fig. 1 March 2007 aerial photograph of the 23-ha study area (demarcated by *bold line*) within the Arizona State University—Tempe campus (*top*) and 3-d model of the study area generated by Arcview 9.3 (*bottom*)

The TR-72U sensors were subject to pre- and post-fieldwork calibration to ensure that measurements were within the manufacturer's specifications.

The traverse occurred during the early morning (0530–0630 hours) on October 28, 2007, as large magnitudes of ΔT_{u-p} are expected a priori during minimum temperature conditions given the open grass park that constitutes most of the SRC field. Cloud-free skies and generally low E winds of 0.4–0.8 ms^{-1} at 10 m above surface level were recorded during the traverse, which minimized the meteorological impacts on both the PCI and UHI (Spronken-Smith and Oke 1998). These ambient weather conditions near the study area were recorded at the Tempe meteorological station of the Maricopa County Air Quality Department (MCAQD). The station was directly adjacent to an ~8-ha park mostly consisting of irrigated lawn grass and was located within a low-density suburban residential neighborhood with predominant mesic landscaping ~670 m SSW of the SRC field. We therefore assumed the station data to be representative of the general near-surface meteorological conditions of our study area. Hourly temperatures from the MCAQD Tempe station were used to obtain time-series data for the study area. The study took place during a night when the SRC field was not irrigated,

Fig. 2 Map of traverse route and classification of different surface types within the study area

although we could not ascertain if other smaller green spaces within the study area were watered.

We recorded ~3,100 temperature datum points per sensor during the traverse, resulting in a total of ~12,400 points for all four sensors. These data were consequently geo-referenced into the previously created GIS model for data analysis. Each datum point could therefore be categorized with its respective surface classification (Table 1). Mean temperatures for each sampling point were derived, together with mean vertical lapse rates for each urban and non-urban surface type.

Table 1 Surface characteristics for classification of traverse data

Land use type	Description of surface over which sampling occurred	No. of traverse sampling points
Urban surfaces		
Asphalt	Dark-colored road surfaces, mainly used by vehicular traffic	1,110
Concrete	Lighter-colored pavement used by pedestrians	1,021
Tennis courts	Hardcourt green colored surface composed of asphalt with rubber compound for cushioning	243
Urban canyons	Urban surface confined within buildings with restricted exposure to sky; minimum (mean) sky view factor is 0.5 (0.7)	281
Rural surfaces		
Xeric	Surface with exposed sandy–loam soil without lawn cover	74
Lawn	Surface planted with lawn grass (bermuda or ryegrass species)	612

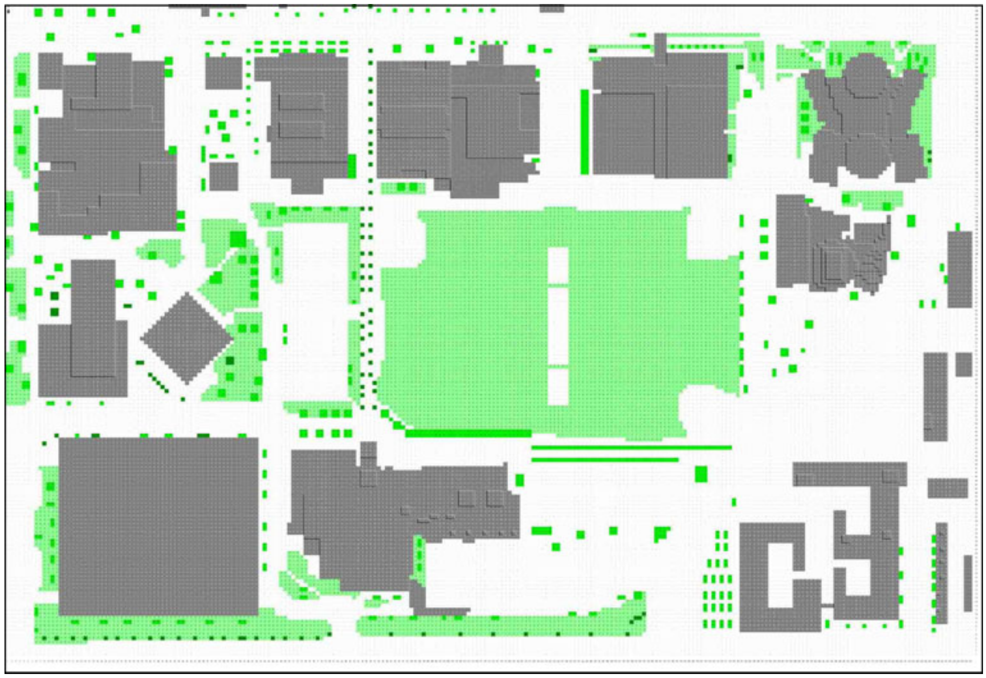

Fig. 3 Part of the area input file for ENVI-met simulations which was based on Figs. 1 and 2. Individual grid cell size was 2.5 × 2.5 × 5 m

3.3 Microclimate model simulation

We selected the ENVI-met urban microclimate model (version 3.1, available as freeware for MS Windows at http://www.envi-met.com) to simulate soil, surface, and vegetation interactions within the urban canopy layer (i.e., below mean roof height). It is a 3-d, non-hydrostatic, prognostic numerical model based on fundamental fluid dynamics and thermodynamic laws (Bruse and Fleer 1998). Typical horizontal resolutions are 0.5–10 m, and simulations are normally run for 24–48 h, with a maximum time step of 10 s (Bruse, 2010). Analysis of small-scale physical interactions between individual buildings, surfaces, soils, and vegetation is thus possible at these modeled spatial and temporal resolutions.

The model requires a user-specified area input file that defines the 3-d geometry of the model environment such as individual buildings and building heights, vegetation, soil and surface types, etc. (Fig. 3), which were derived from Figs. 1 and 2. Although simulated concrete and asphalt surfaces in Fig. 2 could be input into the model, a modeled surface type similar to the tennis court surface could not be found; instead, grid cells with this surface were classed as concrete surfaces. We also selected a relatively high resolution for individual grid cells (2.5 × 2.5×5 m) to complement the observed temperature data resolution. The

Table 2 Observed LAD data for selected trees within the study area

Common name	Species	LAD_{max} (standard error) ($m^2 m^{-3}$)	LAD_{max} height (m)	Mean tree height (m)
Bottle tree	*Brachychiton populneus*	3.23 (0.12)	2.25	7.75
Seville sour orange	*Citrus aurantium*	4.83 (0.18)	0.5	5
Coolibah	*Eucalyptus microtheca*	2.59 (0.13)	2.75	8.75
Shamel ash	*Fraxinus uhdei*	2.46 (0.35)	3	12
White mulberry	*Morus alba*	3.77 (0.14)	2.75	9
Thornless mesquite	*Prosopis hybrid*	2.92 (0.11)	2.5	9
Blue palo verde	*Parkinsonia florida*	1.85 (0.13)	2	7.5
Southern live oak	*Quercus virginiana*	3.02 (0.09)	3	9.25
African sumac	*Rhus lancea*	4.39 (0.24)	2.25	8.25
European olive	*Olea europaea*	3.39 (0.14)	2.25	8.25
Chinese pistache	*Pistacia chinensis*	2.79 (0.11)	1.75	4.5
Aleppo pine	*Pinus halepensis*	2.68 (0.18)	2	4.75
Chinese elm	*Ulmus parvifolia*	1.68 (0.12)	2.75	8.5

area input file was nested within four nesting grids (with the predominant soil type) for numerical stability during model runs. We initially used the vegetation database included in the model defaults when configuring the area input file; however, these database characteristics, such as for normalized vegetation leaf area density data (LAD), were based on temperate forest and crop stands (M. Bruse, personal communication), which have little relevance to the vegetation types found within an arid city. We therefore surveyed vegetation within the study area to empirically estimate leaf area density based on field observations with a Li-Cor LAI-2000 plant canopy analyzer (http://www.licor.com/) and derived vertical leaf area density for each vegetation species based on the method proposed by Lalic and Mihailovic (2004) (Table 2). These database alterations subsequently allowed for input of local vegetation into ENVI-met.

Apart from these vegetation data, the model also required local soil, meteorological, and building input parameters (Table 3) for model initialization. Temperature and relative humidity (RH) at 2 ma.s.l., 10 ma.s.l. wind speed, and direction data from the MCAQD Tempe station were used as initial model inputs, together with soil temperature and soil RH data from the Mesa station of the Arizona Meteorological network (hourly data are available at http://ag.arizona.edu/AZMET/). This station was ~6.5 km away from the SRC field and assumed to have similar soil profiles to the study area (i.e., sandy–loam soils). Specific humidity at 2,500 ma.s.l. was estimated via data from the NCEP/NCAR reanalysis project at the NOAA/ESRL Physical Sciences Division (http://www.cdc.noaa.gov/data/reanalysis/reanalysis.shtml). Lastly, building interior temperatures, mean heat transmission (i.e., thermal conductivity divided by mean wall or roof width), and roof/wall albedo values were estimated from existing table-base data (e.g., Oke 1987) and from field reconnaissance observations.

We ran a model simulation for 24 h starting from sunrise (0600-0600 hours; Oct 27–28, 2007) with updated surface data every 60 s. We subsequently analyzed model output at 0530 hours, coinciding with the start of the bicycle traverse. Modeled potential temperatures at 0 (surface), 1, 2, and 3 m were extracted as geo-referenced (*x*–*y* coordinate reference) text-based .dat files using the accompanying LEONARDO program (V 3.75 Beta) in the ENVI-met software package and were converted to absolute temperatures using Poisson's equation. Using the ASCII to raster tool in ArcView 9.3 GIS software, these files were converted and entered as raster files with 2.5-m *x*–*y* grid cells. The raster files were geo-referenced with the other map layers; warm features of the model output, i.e., buildings, were prominent in the raster and created excellent spatial references. This geo-referencing had an average root mean square error (RMSE) of 1.45 m; this error was both unavoidable and systematic and is the result of 2.5-m gridded layers being geo-referenced to a discrete continuous map surface. Following geo-referencing, the raster grid was converted to a polygon feature class so that it could be spatially joined with the observed sample point layer. In this manner, each of the ~3,100 datum points at the 0.01-, 1-, 2-, and 3-m

Table 3 Selected input parameters for ENVI-met simulations

Category	User input during simulations
Meteorological inputs	
Wind speed and direction 10 m above ground	0.8 ms^{-1}/85°
Approximate roughness length of study area	0.5 m
Specific humidity at 2,500 ma.s.l.	2.75 g/kg
Relative humidity at 2 ma.s.l.	20%
Initial atmospheric temperature	290.3 K
Soil inputs	
Initial soil temperature at upper layer (0–20 cm)	293 K
Initial soil temperature at middle layer (20–50 cm)	294 K
Initial soil temperature at lower layer (below 50 cm)	295 K
Relative humidity, upper layer	25%
Relative humidity, middle layer	30%
Relative humidity, lower layer	35%
Building inputs	
Building interior temperature	303 K
Mean heat transmission[a] of walls	1.7 $Wm^{-2}K^{-1}$
Mean heat transmission of roofs	6.0 $Wm^{-2}K^{-1}$
Mean wall albedo	0.3
Mean roof albedo	0.4

[a] Estimated thermal conductivity of building material (Wm^{-1} K^{-1}) divided by mean wall thickness (m)

elevations could be directly compared with the corresponding ENVI-met model output.

4 Results

4.1 PCI effect—observations and modeling

Both data from the bicycle traverse and from the ENVI-met simulations illustrated a distinct PCI that developed over the SRC field. Observed temperatures from 0.01- and 2-m heights showed the SRC field and the adjacent west tennis court as having cooler temperatures compared to the surrounding buildings, pavements, and urban canyons (Fig. 4). Temperatures at 2-m heights were also generally warmer when compared to the surface, especially over the lawn and xeric surfaces. The approximate maximum difference in temperature at 0.01 m (2 m) between the SRC field and its urban surroundings was ~5.8°C (3.1°C), although there were relatively large variations in temperature over the urban surfaces adjacent to the field. We observed notable temperature differences within the field, with a cooler "core" in its center compared to its warmer perimeter adjacent to concrete or asphalt surfaces. Slightly cooler urban temperatures were observed W of the field and tennis courts, possibly indicating the effect of advection from easterly wind flow, with urban canyon temperatures in the western section of the study generally being ~1°C cooler compared to the eastern section.

Simulated temperatures from ENVI-met also showed a PCI, albeit with lower approximate maxima of 3.6°C and 2.9°C at surface and 2-m heights, respectively. Cooler temperatures were observed over the field and tennis courts, and a similar shift of cold air from advection from E to W was present (Fig. 5). Temperatures at the surface were generally cooler than at 2-m heights, with lower temper-

Fig. 4 Temperatures observed from traverse for 0.01- (*top*) and 2-m heights (*bottom*) from 0530–0630 hours

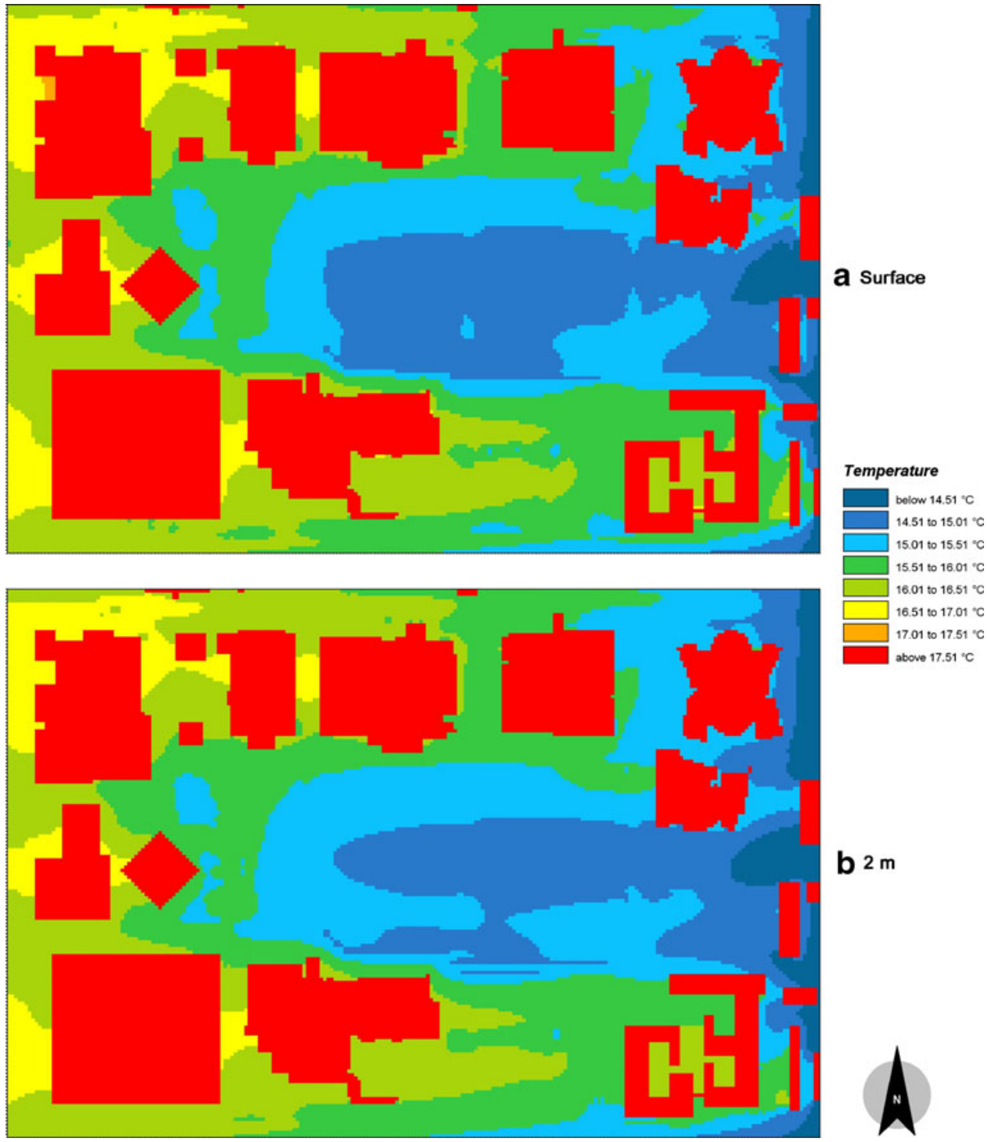

Fig. 5 2-d profiles of ENVI-met temperature simulations for surface (**a**) and 2-m levels (**b**) at 0530 hours

atures at the center of the SRC lawn field as compared to its xeric surfaces. Colder temperatures were present along the eastern part of the study area, in contrast to observed temperature data, but this was most likely a consequence of the model's nesting grids of sandy–loam soils along its boundaries coupled with the constant E wind flow during the simulation period. Pockets of warmer air were observed within urban canyons in the western part of the study area, especially within N–S-orientated canyons, which possibly resulted as a lee effect from buildings acting as windbreaks and impeding the advection of cooler air from the park.

4.2 Variations of PCI intensity and vertical lapse rates over different surfaces

We examined variations in $\Delta T_{u\text{–}p}$ over different heights for both modeled and observed data from the surface up to 3 m. Magnitudes of mean PCI were defined as the difference in temperatures between each mean urban (i.e., asphalt, concrete, tennis courts, and urban canyons) vs. non-urban surface (i.e., lawn or xeric) for all heights (Table 4). Mean observed PCI intensities ranged from 1.4 to 3.8°C with magnitudes decreasing significantly with increasing observation height for all surface types. For example, mean $\Delta T_{\text{urban-non-urban}}$, derived by the difference between mean urban and non-urban surfaces, was 2.6°C less at screen-level heights of 2 m vs. 0.01 m. Mean ENVI-met PCI intensities were, however, generally lower in magnitude at all comparative heights, especially between the surface and 1-m heights, although qualitative differences (i.e., ranking of PCI intensities between surface types) are largely similar between observed and modeled $\Delta T_{u\text{–}p}$.

Different surface types influenced urban vs. non-urban lapse rates. Vertical distribution of mean temperatures measured over asphalt, concrete, and within urban canyons

Table 4 Mean PCI (ΔT_{u-p}) over different surface types from observed and modeled data

PCI by surface type (m)	0	0.01	1	2	3
Mean temperature from traverse observations (°C)					
Concrete—xeric		2.4	1	0.7	0.5
Concrete—lawn		3.8	1.3	1.1	0.9
Asphalt—xeric		2.3	1.1	0.7	0.5
Asphalt—lawn		3.7	1.4	1.1	0.9
Urban canyon—xeric		2.3	1.1	0.7	0.4
Urban canyon—lawn		3.7	1.4	1.1	0.8
Tennis court—xeric		1.4	0.2	0	0
Tennis court—lawn		2.8	0.5	0.4	0.4
Mean urban − mean non-urban		3.6	1.4	1.0	0.7
Mean temperature from model simulations (°C)					
Concrete—xeric	0.43		0.37	0.34	0.32
Concrete—lawn	0.83		0.75	0.70	0.65
Asphalt—xeric	0.49		0.45	0.41	0.38
Asphalt—lawn	0.89		0.83	0.77	0.71
Urban canyon—xeric	0.78		0.75	0.72	0.70
Urban canyon—lawn	1.18		1.13	1.08	1.03
Tennis court—xeric	0.15		0.11	0.08	0.05
Tennis court—lawn	0.55		0.49	0.44	0.38
Mean urban − mean non-urban	0.82		0.75	0.70	0.65

Heights are above surface level

showed insignificant changes at all heights (Fig. 6); however, similar profiles over tennis court surfaces were generally ~1°C less compared to other urban surface types. This influences PCI intensity, with $\Delta T_{\text{tennis courts–xeric}}$ equal to zero at both 2 and 3 m (Table 4). There were also important differences of PCI intensity with respect to non-urban surfaces, as ΔT_{u-p} having consistently greater magnitudes when measured over lawn as opposed to xeric surfaces, with higher intensities documented closer to the ground. An analysis of the observed vertical lapse rates showed significant differences of stability between urban and non-urban surfaces. Asphalt, concrete, tennis court, and urban canyon surfaces generally had near-neutral or slightly stable conditions from 0 to 2 m, but non-urban xeric and lawn surfaces had a strong inversion observed at those heights, especially from 0 to 1 m (Fig. 6). Above 2 m, however, all surfaces had neutral to slightly unstable air capping the near-surface inversion.

Modeled lapse rates did not show the stable stratification of observed temperatures; instead, lapse rates were neutral for all surface types from 0 to 3 m, with a much smaller range especially at lower heights. The order of warmer to colder temperature profiles was largely similar to the observed vertical profiles, with lawn surfaces being coldest and urban canyons being warmest. Of note, however, is that the modeled vertical temperature profile within urban canyons had higher temperatures (0.4°C) when compared to asphalt or concrete surfaces, whereas such differences in temperature were negligible during the traverse observations.

4.3 Evaluation of ENVI-met simulations

We evaluated the model's performance in terms of accuracy with observed data in two ways. First, modeled spatial temperatures at 0530 hours were compared with observed traverse data across similar heights. Second, time-series data categorized under different land use categories at 2 m were averaged and subsequently compared with similar data from the nearby MCAQD Tempe station. In this study, we used several absolute quantitative difference measures of mean bias error (MBE), mean average error (MAE), RMSE, and its derived systematic ($RMSE_S$) and unsystematic ($RMSE_U$) components (Willmott 1982). These error indices, together with the relative, dimensionless difference measure of the index of agreement (*d*), are used in conjunction to evaluate the accuracy of ENVI-met temperatures, where accuracy is defined as the degree to which predicted observations (*P*) approach magnitudes of actual observed data (*O*). These measures are preferred to simple correlation measures (e.g., r, r^2) which are completely insensitive to additive and proportional differences that potentially exist between *P* and *O* and thus may not be consistently related to model prediction accuracy. For instance, it is possible for low or even negative measures of *r* simultaneously occurring with relatively small differences between magnitudes of *P* and *O*, if the mean of either one of the variables is stationary and its deviations about that mean are unsystematic (Willmott 1984). Further, utilizing difference or error measures allows for the

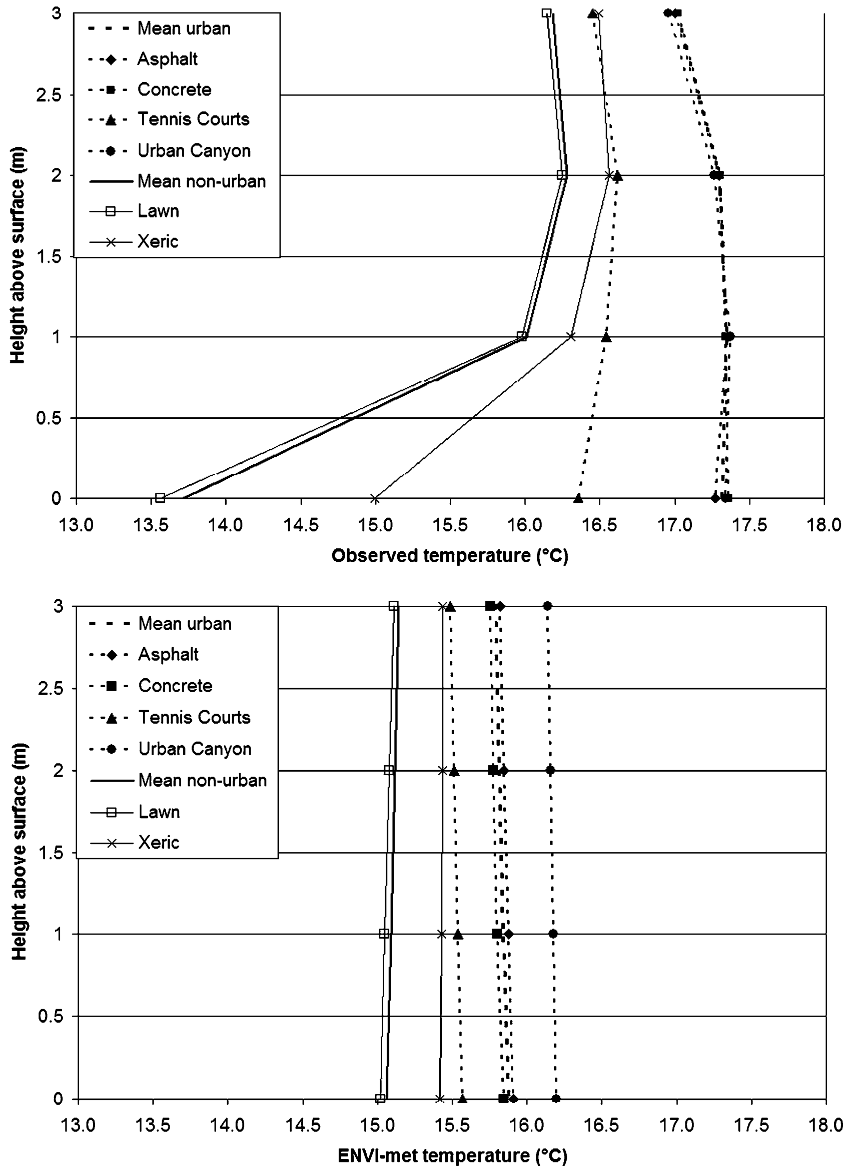

Fig. 6 Mean vertical temperature profiles for each surface from traverse data taken at 0.01, 1, 2, and 3 m above surface level (*top*) and corresponding ENVI-met data at 0, 1, 2, and 3 m above surface level (*bottom*). Urban surface temperatures are the mean profiles of temperatures taken over asphalt, concrete, tennis court, and urban canyon surfaces. Non-urban surface temperatures comprise of the mean xeric and lawn profiles

evaluation of systematic and unsystematic errors within the model, which are not readily available with simple correlation plots of *P* vs. *O*.

Four model levels corresponding to the nearest traverse sensor height were selected for comparison of spatial temperature fields: 0 m (*P*) with 0.01 m (*O*), 1 m (*P*) with 1 m (*O*), 2 m (*P*) with 2 m (*O*), and 3 m (*P*) with 3 m (*O*) data. The comparison between surface and 0.01-m data may be complicated by observed raised temperature minima over a variety of surfaces (Oke 1970; Geiger et al. 2003), but we assume that these differences are relatively insignificant between 0 and 0.01 m, especially over vegetated areas (e.g., short grass lawns) that have raised active surfaces>0.01 m generally documented under clear and windless weather conditions (Oke 1987).

The MBE for all comparisons show that the model generally under-predicted temperatures by 0.74–1.38°C (Table 5). MAE ranged from 1.16 to 1.47°C, with a larger error occurring closer to the surface. The magnitudes of RMSE for all heights were relatively low (<1.7°C), but a decomposition of RMSE indicates that a systematic error predominates. A probable source of this would be the cooler temperatures consistently simulated along the eastern, urban part of the study area (Fig. 5), which is in contrast to the warmer temperatures observed during the traverse (Fig. 4). A possible explanation could lie in how the model parameterizes lateral boundary conditions for both surfaces and turbulent inflow. The use of open lateral boundaries, coupled with the study area being nested within grids of sandy–loam soils, allows for the constant flow of easterly winds to advect cooler air into the model's eastern boundary. Further, the observed temperature data may be subject to sensor lag in some areas of stagnant turbulence, which affects a key assumption that observed data are error-free in

Table 5 Difference measures of ENVI-met model temperatures with observed temperature data at 0530 hours

Height of ENVI-met model simulation				
Difference measure (unit)	Surface[a]	1 m	2 m	3 m
MBE (°C)	−0.74	−1.33	−1.38	−1.16
MAE (°C)	1.47	1.33	1.38	1.16
RMSE (°C)	1.63	1.50	1.53	1.31
$RMSE_S$ (°C)	1.49	1.32	1.37	1.24
$RMSE_U$ (°C)	0.67	0.71	0.69	0.69
d (dimensionless)	0.57	0.47	0.41	0.40

[a] Surface model data are compared with observed 0.01 m data

the statistical analysis via difference measures. Another potential error in the observed data could lie with the systematic errors from the spatial join process described in "Section 3.3", which could propagate additional unavoidable systematic errors. Despite these factors, the relatively low error indices, combined with acceptable magnitudes of *d* (0.4–0.57) given the systematic errors present, suggest that the model reasonably approximates the spatial distribution of temperatures and derived $\Delta T_{u\text{–}p}$.

The time-series data for mean modeled 2-m temperatures over all surfaces compared favorably with 2-m temperature data obtained from the MCAQD Tempe weather station (Fig. 7). The model generally under-predicted (over-predicted) nocturnal (daytime) temperatures, which are similar patterns documented in previous applications of ENVI-met (e.g., Emmanuel and Fernando 2007). During the day, mean temperatures over asphalt surfaces were systematically and significantly higher vs. that of other surfaces, probably due to its larger (lower) heat capacity (heat conductivity) relative to other surface materials. It is also notable that these modeled mean near-surface temperatures over asphalt cooled more than other urban surfaces after sunset. $RMSE_S$ (2.23°C) was slightly greater than $RMSE_U$ (1.95°C), which could be a consequence of several limitations of ENVI-met, such as its inability to (a) dynamically simulate heat storage for building walls and roofs by having constant building indoor temperatures with no thermal mass and (b) simulate regional-scale thermal and turbulence exchanges that may directly influence micro-scale climates. The latter point can be illustrated with the sudden increase in temperature in the MCAQD data from 0300 to 0400 hours, which could have resulted from the advection of warmer air from adjacent urban areas due to the nocturnal near-surface transition (Brazel et al. 2005). Despite these limitations, the relatively low RMSE and MAE, coupled with the high *d*, suggest that the model is accurate in simulating time-series temperature data for this study.

5 Discussion

5.1 Surface controls on PCI intensity

Compared to results from other studies (e.g., Spronken-Smith and Oke 1998; Jonsson 2004), mean PCI ($\Delta T_{u\text{–}p}$)

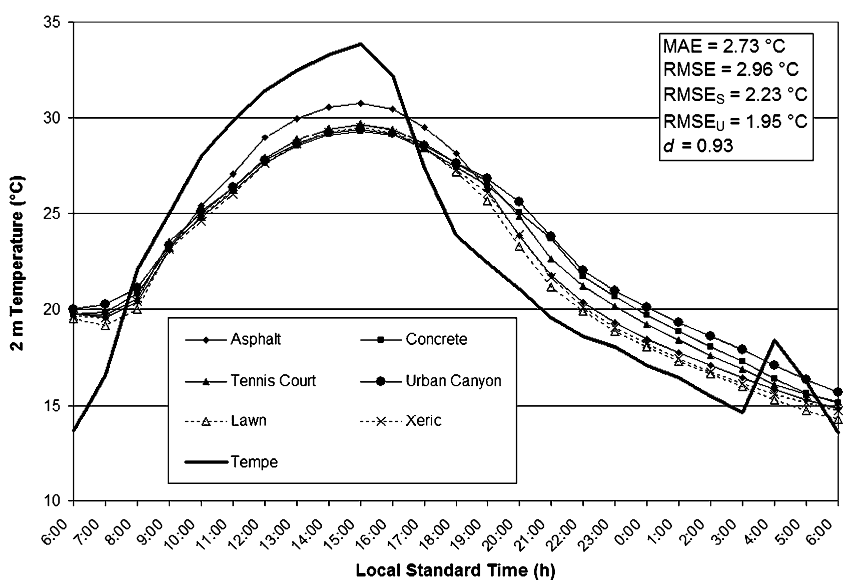

Fig. 7 Mean 2-m temperatures from ENVI-met simulations over different land use types (see Table 1) and from MCAQD Tempe meteorological station over a 24-h period from Oct 27 to 28, 2007. Difference measures are for mean modeled 2-m temperatures across all surfaces vs. MCAQD 2-m temperatures

intensities documented in this present study are similar in magnitude, i.e., between 0.7 and 3.6°C. There are large variations in ΔT_{u-p} between heights, with both the observed and modeled PCI intensities being larger at heights closer to the surface (Table 3; Fig. 6). Possible explanations for these results are now discussed.

As observations were conducted under mostly ideal meteorological conditions (i.e., clear and mostly calm weather), which largely preclude the turbulent transfer of sensible and latent heat fluxes, the large differences of observed temperature magnitudes at 0.01-m heights between urban and non-urban surfaces are probably due to variations of net long-wave radiation losses. These relatively strong upward radiative fluxes occur close to the surface, as seen from the strong temperature gradient between 0 and 1 m, especially over xeric and lawn surfaces (Fig. 6). This surface flux divergence probably causes the strong non-urban surface inversions compared to the near-neutral lapse rates observed over urban surfaces.

The radiative losses are controlled by the varying thermal responses of different surface materials, which can be quantified by μ and/or moisture availability. Generally, surfaces with high μ, such as concrete or asphalt, release stored heat at slower rates and would remain warmer at sunrise compared to soil or lawn surfaces (e.g., Oke 1987). Lower temperatures measured over tennis courts could thus be explained by the lower μ on this surface. Likewise, differences in 0.01-m temperatures between xeric and lawn surfaces probably arise from μ variations, with lawn surfaces having lower μ values corresponding to lower surface temperatures. Another possible influence, however, would be deviations in non-urban soil moisture content. Two possible impacts on temperature may arise. First, higher (lower) soil moisture results in higher (lower) μ and has been shown to reduce urban vs. non-urban temperature differences (Chow and Roth 2006). Second, given the study area's arid climate and the strong surface-atmosphere vapor pressure deficit, greater soil moisture would likely result in greater cooling due to increased evapotranspiration, which a priori is more likely to occur over lawns than xeric surfaces. The relative importance of these two impacts is unknown and would require a further process-based study, although Spronken-Smith and Oke (1999) suggested that cooling from evapotranspiration of soil moisture is more significant at pre-sunset, while the additional soil wetness would inhibit nocturnal cooling due to increased μ based on scale and numerical modeling evaluations.

Another possibility explaining the variance in urban temperatures could be the relatively larger sky view factor associated with the exposed tennis courts. The geometry of urban canyons have been shown to influence temperatures and cooling rates with respect to urban parks (Upmanis et al. 1998), and the lack of urban canyons on tennis courts results in unhindered radiative cooling and cooler temperatures. The small but significant variation in modeled ENVI-met lapse rates between "tennis courts" (which are simulated concrete surfaces) and concrete and urban canyon surfaces (Fig. 6) further suggests that changes in urban geometry could be a likely factor in explaining intra-urban temperature differences. However, the lack of significant differences in observed lapse rates within urban canyons vs. exposed concrete and asphalt surfaces implies that the impact of urban geometry on temperatures may be superseded by other larger-scale influences not modeled by ENVI-met.

5.2 Surface/lapse rates relationships and advection

Results from observed lapse rate data in this study are qualitatively similar with the only known previous PCI study that examined vertical temperature differences for urban green spaces in Stockholm, Sweden (Jansson et al. 2007), with generally neutral/near-neutral (stable) urban (non-urban) profiles observed in both cities. A significant difference lies in the magnitude of profile stability for non-urban surfaces between studies. In Stockholm, the maximum increase in vertical temperatures within a park was ~1.5°C from 0.47 to 2.47 m at 2200 hours LT, compared to 2.2°C (1.4°C) between 0 and 3 m for lawn (xeric) surfaces in this study (Fig. 6). Variations in green space type (i.e., lawn/xeric vs. trees), timing of observations (i.e., early evening vs. pre-dawn), and site micro-climates (i.e., different wind speeds and climate types) may help to explain these differences in lapse rate magnitudes. Of more interest is that, although the near-neutral vertical lapse rate simulations in ENVI-met from 1 to 4 m were qualitatively similar to observed data, the strong stability over lawn and xeric surfaces between 0 and 1 m was not well modeled, leading to a large under-estimation of simulated ΔT_{u-p} within these heights. Whether this is due to inadequate model surface and soil parameterization or from limitations of modeled surface–atmospheric physics is still unknown and requires further investigation.

The Jansson et al. (2007) study also postulated that advection, possibly generated by pressure gradient from temperature differences between park and non-park surfaces, likely factored in decreases in PCI intensity with height. These local-scale nocturnal "park breezes" of low wind speed (~0.5 ms^{-1}) were observed in Göteborg under clear and calm weather (Eliasson and Upmanis 2000) and could have occurred near the SRC field in this study. Although the lower 0.01-m temperatures at tennis courts relative to other urban surfaces were probably due to its different surface characteristics, its low 1- to 3-m temperatures were likely affected by the advection of the cooler air mass from the adjacent SRC field, which can be discerned from Figs. 4 and 5. It is very likely that this advection extended the PCI effect westward, possibly by the width of the park itself (~ 200 m) as suggested by Spronken-Smith and Oke (1998). However, the prevailing easterly winds observed here were similar in direction to the expected E–W evening transition, which affects most of the Phoenix metropolitan area by sunrise (Brazel et al. 2005). It was thus possible that the shift of cooler air over the SRC field during the early morning was driven by this larger-scale synoptic turbulent process and could have masked potential park breezes. Further PCI observations, especially during the early evening hours during the incipient stages of the evening transition in Phoenix, are needed to determine if park breezes develop in the study area.

6 Conclusion

This study investigated the micro-scale impacts of an urban green space on temperatures located within a hot, arid city. We obtained pre-sunrise temperature data of high spatial and temporal resolution from a bicycle traverse as well as from simulations from a numerical micro-scale climate model (ENVI-met 3.1). Examination and discussion of horizontal and vertical temperature distributions revealed the following results:

- A strong PCI effect was evident over a large park consisting of irrigated lawn grass and bare soil (xeric) areas. Mean (maximum) observed PCI intensities (i.e., ΔT_{u-p}) were ~3.5°C (~6°C) depending on the urban and non-urban surface category, with larger PCI magnitudes documented closer to the surface, especially between 0- and 1-m heights. Surface type affected PCI intensities, with observed larger ΔT_{u-p} occurring over irrigated lawn as opposed to xeric surfaces, and it is likely that soil moisture and surface thermal properties are likely factors that explain this variance. Urban surfaces more exposed to the atmosphere (i.e., with higher sky view factors) also had observed lower PCI intensities when compared to surfaces within urban canyons.
- A strong inversion layer was detected over non-urban surfaces, especially between 0- and 1-m heights, which probably resulted from intense surface radiative cooling from non-urban surfaces. Magnitudes of this near-surface vertical cooling (2.2°C for lawn surfaces from surface to 1 m) are much greater than that reported for a PCI in a high-latitude city (Jansson et al. 2007).
- Spatial and time-series data from the ENVI-met model were evaluated using a suite of difference measure indices of predicted vs. observed temperatures, which are considered a more preferable statistical method for determining model accuracy as opposed to simple correlation measures. The model reasonably simulated mean spatial temperature fields, especially in areas not directly adjacent to model boundaries that increased systematic errors. However, the model did not simulate the strong near-surface inversion over non-urban surfaces. A comparison with mean 2-m temperature time-series data at a nearby meteorological station demonstrated a much higher accuracy of mean modeled data, even after accounting for the lack of regional exchange processes that were not simulated in the micro-scale ENVI-met model.
- Advection of colder park air towards urban surfaces, combined with an increased surface exposure to the atmosphere, may be important factors in explaining cooling at different heights over adjacent urban surfaces. Both the modeled and observed results showed that the PCI effect at 2- and 3-m heights over several tennis courts next to the lawn/xeric field was either negligible or non-existent depending on the park surface type. Steady E winds, combined with high sky view factors at the tennis courts, are probable causes for this result. Urban canyons perpendicular to the prevailing wind had lee effects that manifest as higher observed and modeled temperatures.

Results from this study show that, for arid cities, the PCI developed over irrigated lawn and xeric surfaces can be of sufficient magnitude to mitigate the strong UHI in Phoenix, especially within the urban canopy layer (e.g., Brazel et al. 2007). Advection of cooler park air and building orientation are also important factors in variations of PCI over space within the study area; urban planners and builders should be cognizant of these issues when examining how green spaces can mitigate the UHI. Lastly, although the ENVI-met model does have relatively larger systematic vs. unsystematic errors, this study shows that its accuracy of observed spatial and time-series data is relatively reasonable, and it has the potential to be utilized as an effective planning tool for modeling micro-scale climates in Phoenix, especially after adapting several vegetation and soil parameters to local conditions

Acknowledgements The authors would like to thank Thomas K. Swoveland, Abeer Hamdan and Paul Iñiguez (Arizona State University) for their assistance during fieldwork reconnaissance and data collection. Dr. Chen-Yi Sun (National Chin-Yi University, Taiwan) and Dr. Nancy Selover (Office of the Arizona State Climatologist) advised on the instrument and measurement techniques. Dr. Jianguo Wu (Arizona State University) and Dr. Michael Bruse (Johannes Gutenberg-Universität Mainz) provided critical feedback and comments. We also thank the Maricopa County Air Quality Department for providing secondary climate data from the Tempe meteorological station. This material is based upon work supported by the National Science Foundation under Grant No. DEB-0423704, Central Arizona - Phoenix Long-Term Ecological Research (CAP LTER). The lead author was also supported by the Department of Geography, National University of Singapore.

References

Barradas VL (1991) Air temperature and humidity and human comfort index of some city parks of Mexico City. Int J Biometeoro 35:24–28

Brazel AJ, Fernando HJS, Hunt JCR, Selover N, Hedquist BC, Pardyjak E (2005) Evening transition observations in Phoenix, Arizona. J Appl Meteor 44:99–112

Brazel AJ, Gober PA, Lee SJ, Grossman-Clarke S, Zehnder J, Hedquist B, Comparri E (2007) Determinants of changes in the regional urban heat island in metropolitan Phoenix (Arizona, USA) between 1990 and 2004. Clim Res 33:171–182

Bruse M (2010) ENVI-met 3.1: model overview. University of Bochum. Available at: www.envi-met.com

Bruse M, Fleer H (1998) Simulating surface–plant–air interactions inside urban environments with a three dimensional numerical model. Environ Model Softw 13:373–384

Chow WTL, Roth M (2006) Temporal dynamics of the urban heat island of Singapore. Int J Climatol 26:2243–2260

Eliasson I, Upmanis H (2000) Nocturnal airflow from urban parks—implications for city ventilation. Theor Appl Climatol 66:95–107

Emmanuel R (2005) An urban approach to climate-sensitive design: strategies for the tropics. Spon, New York

Emmanuel R, Fernando HJS (2007) Urban heat islands in humid and arid climates: role of urban form and thermal properties in Colombo, Sri Lanka and Phoenix, USA. Clim Res 34:241–251

Garcia-Cueto R, Jauregui E, Tejeda A (2003) Urban/rural energy balance observations in a desert city in northern Mexico. In: Proceedings of Fifth International Conference on Urban Climate, Lodz, Poland, 177–180

Geiger R, Aron RH, Todhunter P (2003) The climate near the ground, 6th edn. Rowman & Littlefield, Lanham, Maryland

Gober P (2006) Metropolitan Phoenix: place making and community building in the desert. University of Pennsylvania Press, Philadelphia

Grimmond CSB, Oke TR (1995) Comparison of heat fluxes from summertime observations in the suburbs of four North American cities. J Appl Meteorol 34:873–889

Jansson C, Jansson P-E, Gustafsson D (2007) Near surface climate in an urban vegetated park and its surroundings. Theor Appl Climatol 89:185–193

Jauregui E (1990/1991) Influence of a large park on temperature and convective precipitation in a tropical city. Energ Buildings 15–16:457–463

Jonsson P (2004) Vegetation as an urban climate control in the subtropical city of Gaborone, Botswana. Int J Climatol 24:1307–1322

Kirby SF, Sellers WD (1987) Cold air drainage and urban heating in Tucson, Arizona. J Arizona Nevada Acad Sci 22:123–128

Kurn D, Bretz S, Huang B, Akbari H (1994) The potential for reducing urban air temperatures and energy consumption through vegetative cooling. ACEEE Summer Study on Energy Efficiency in Buildings, American Council for an Energy Efficient Economy. Pacific Grove, California. Available at http://www.osti.gov/bridge/servlets/purl/10180633-hLSlld/native/10180633.PDF. Accessed 23 Jul 2009

Lalic B, Mihailovic DT (2004) An empirical relation describing leaf-area density inside the forest for environmental modeling. J Appl Meteorol 43:641–645

Martin CA (2008) Landscape sustainability in a Sonoran desert city. Cities Envir 1(2):1–16

Muellar EC, Day TA (2004) The effect of urban groundcover on microclimate, growth and leaf gas exchange in oleander in Phoenix, Arizona. Int J Biometeor 49:244–255

Oke TR (1970) The temperature profile near the ground on calm clear nights. Q J Roy Meteor Soc 96:14–23

Oke TR (1987) Boundary layer climates. Methuen, New York, p 372

Oke TR (1989) The micrometeorology of the urban forest. Phil Trans R Soc Lond B324:335–349

Oke TR (2004) Initial guidance to obtain representative meteorological observations at urban sites. Instruments and methods of observation program. IOM report no. 81, WMO/TD 1250, World Meteorological Organization, Geneva

Oke TR, Johnson GT, Steyn DG, Watson ID (1991) Simulation of surface urban heat islands under "ideal" conditions at night. Part 2: diagnosis of causation. Bound-Layer Meteor 56:339–359

Pearlmutter D, Berlinera P, Shaviv E (2007) Urban climatology in arid regions: current research in the Negev desert. Int J Climatol 27:1875–1885

Pearlmutter D, Krüger EL, Berlinera P (2009) The role of evaporation in the energy balance of an open-air scaled urban surface. Int J Climatol 29:911–920

Roth M, Oke TR, Emery WJ (1989) Satellite-derived urban heat islands from three coastal cities and the utilization of such data in urban climatology. Int J Remote Sens 10:1699–1720

Saito I, Ishihara O, Katayama T (1990/1991) Study of the effect of green areas on the thermal environment in an urban area. Energ Buildings 15–16:493–498

Sham S (1987) Urbanization and the atmospheric environment in the low tropics: experiences from the Kelang Valley Region. Malaysia Universiti Kebangsaan Malaysia, Bangi

Shashua-Bar L, Pearlmutter D, Erell E (2009) The cooling efficiency of urban landscape strategies in a hot dry climate. Landscape Urban Plan 92:179–186

Souza LCL, Rodrigues DS, Mendes JFG (2003) Sky view factors estimation using a 3D-GIS extension. Eighth International IBPSA Conference, Eindhoven, Netherlands. August 11–14, 2003. Available at www.ibpsa.org/proceedings/BS2003/BS03_1227_1234.pdf (accessed 23 Jul 2009)

Spronken-Smith RA (1994) Energetics and cooling in urban parks. Unpublished PhD thesis. The University of British Columbia, Vancouver

Spronken-Smith RA, Oke TR (1998) The thermal regime of urban parks in two cities with different summer climates. Int J Remote Sens 19:2085–2104

Spronken-Smith RA, Oke TR (1999) Scale modelling of nocturnal cooling in urban parks. Bound-Layer Meteor 93:287–312

Spronken-Smith RA, Oke TR, Lowry WP (2000) Advection and the surface energy balance of an irrigated urban park. Int J Climatol 20:1033–1047

Stabler LB, Martin CA, Brazel AJ (2005) Microclimates in a desert city were related to land use and vegetation index. Urban For Urban Gree 3:137–147

Sun CY, Brazel AJ, Chow WTL, Hedquist BC, Prashad L (2009) Desert heat island study in winter by mobile transect and remote sensing techniques. Theor Appl Climatol 98(3–4):323–335. doi:10.1007/s00704-009-0120-2

Upmanis H, Eliasson I, Lindqvist S (1998) The influence of green areas on nocturnal temperatures in a high latitude city (Göteborg, Sweden). Int J Climatol 18:681–700

Willmott CJ (1982) Some comments on the evaluation of model performance. Bull Am Meteor Soc 63(11):1309–1313

Willmott CJ (1984) On the evaluation of model performance in physical geography. In: Gaile GL, Willmott CJ (eds) Spatial statistics and models. D Reidel, Dordrecht, pp 443–460

Wong NH, Jusof SK (2008) GIS-based greenery evaluation on campus master plan. Landsc Urban Plan 84(2):166–182